ONCOIMMUNOLOGY
2024, VOL. 13, NO. 1, 2316945
https://doi.org/10.1080/2162402X.2024.2316945

A bispecific anti-PD-1 and PD-L1 antibody induces PD-1 cleavage and provides enhanced anti-tumor activity

Diana I. Albu, Benjamin J. Wolf, Yan Qin, Xianzhe Wang, Amy Daniel Ulumben, Mei Su, Vivian Li, Eirene Ding, Jose Angel Gonzalo, Jason Kong, Ruturaj Jadhav, Nelly Kuklin, Alberto Visintin, Bing Gong, and Thomas J. Schuetz

Compass Therapeutics Inc, Boston, MA, USA

ABSTRACT

Combinatorial strategies, such as targeting different immune checkpoint receptors, hold promise to increase the breadth and duration of the response to cancer therapy. Here we describe the preclinical evaluation of CTX-8371, a protein construct which combines PD-1 and PD-L1 targeting in one bispecific, tetravalent antibody. CTX-8371 matched or surpassed the activity of anti-PD-1 and PD-L1 benchmark antibodies in several *in vitro* T cell activation assays and outperformed clinically approved benchmarks in the subcutaneous MC38 colon and the B16F10 lung metastasis mouse tumor models. Investigation into the mechanism of action revealed that CTX-8371 co-engagement of PD-1 and PD-L1 induced the proteolytic cleavage and loss of cell surface PD-1, which is a novel and non-redundant mechanism that adds to the PD-1/PD-L1 signaling axis blockade. The combination of CTX-8371 and an agonistic anti-CD137 antibody further increased the anti-tumor efficacy with long-lasting curative therapeutic effect. In summary, CTX-8371 is a novel checkpoint inhibitor that might provide greater clinical benefit compared to current anti-PD-1 and PD-L1 antibodies, especially when combined with agents with orthogonal mechanisms of action, such as agonistic anti-CD137 antibodies.

ARTICLE HISTORY
Received 27 July 2023
Revised 18 January 2024
Accepted 6 February 2024

KEYWORDS
Cancer immunotherapy; immuno-oncology

Introduction

Programmed death protein 1 (PD-1, CD279) is a transmembrane protein expressed by multiple lymphoid and myeloid cells and is upregulated in response to antigenic stimulation in T and B lymphocytes.[1] PD-1 binds to PD-L1 (B7-H1) and PD-L2 (B7-H2), which are expressed by several immune and nonimmune cells including cancer cells. PD-1 delivers an inhibitory intracellular signaling cascade and provides negative feedback to the activated cells.[2–7] While the suppressive activity of PD-1 is necessary to ensure homeostasis and control the tissue destructive potential of cytotoxic cells, it is also a mechanism exploited by cancerous cells to avoid cytotoxic T cell attack.[8,9] FDA-approved mAbs inhibiting the PD-1/PD-L1 signaling axis have been remarkably successful in the clinic,[10–14] however, acquired and intrinsic resistance to immune checkpoint blockade impedes anti-tumor immunity.[15,16] To overcome resistance to checkpoint inhibitors (CPIs) monotherapy, combinations of different CPIs and CPIs plus chemotherapy or radiation have been explored and some, such as Nivolumab with either ipilimumab or relatlimab (anti-LAG-3) are in clinical use. Furthermore, bispecific antibodies with dual-targeting specificities are being developed and several such molecules have already been approved.[17–20] Using the Stitchmab™ platform technology we generated and tested combinations of approved immunomodulatory antibodies in a bispecific format.[21] Stitchmabs of pembrolizumab x atezolizumab and nivolumab x atezolizumab (PD-1 × PD-L1) displayed increased potency over the combined non-linked antibodies in a mixed lymphocyte reaction (MLR), thus providing the rationale to generate anti-PD-1 × PD-L1 bispecific antibodies with suitable pharmaceutical properties. Here we present a comprehensive characterization of CTX-8371, a tetravalent bispecific antibody which blocks the PD-1/PD-L1 pathway by simultaneously binding PD-1 and PD-L1. Investigations into the activity of CTX-8371 revealed a mechanism of action not previously described for PD-1 or PD-L1 CPIs, namely the bispecific antibody-induced proteolytic cleavage of cell surface PD-1.

Methods

Ethics statement

All mandatory laboratory health and safety procedures have been complied with within the course of conducting any experimental work reported. All animal procedures were conducted under Compass Therapeutics IACUC-approved protocol (CTX19–1).

Assessment of CTX-8371 activity *in vitro*

Human PBMCs activated for 72 h with anti-CD3ε and anti-CD28 antibodies (0.25 µg/mL each) or *Staphylococcus aureus* Enterotoxin A (SEA) (Sigma), were incubated with test antibodies for additional 24 h. In some experiments, the next day, cells were washed thoroughly, further incubated with anti-CD3/anti-CD28 for 5 days and

CONTACT Diana I. Albu diana.albu@compasstherapeutics.com Compass Therapeutics Inc, 80 Guest St, Suite 601, Boston, MA 02135, USA
Supplemental data for this article can be accessed online at https://doi.org/10.1080/2162402X.2024.2316945.

sampled daily for Western Blot (WB), FACS, qPCR, or ELISA. In others, parental anti-PD-L1 was added in excess (50 nmol/L) 5 min before addition of CTX-8371. Epoxomicin, (5 µmol/L), chloroquine, or batimastat (Millipore), were added as shown in figures. In kinetic experiments, human PBMCs were activated for 72 h with anti-CD3ε and anti-CD28 antibodies in the presence of test antibodies. For PDCD1 gene expression, human PBMCs activated for 72 h with anti-CD3ε and anti-CD28 antibodies (0.25 µg/mL each) were washed and cells incubated with test antibodies for additional 24 h. For MLR, $CD4^+$ T cells and $CD14^+$ monocytes were isolated from PBMCs of two donors by Dynabeads (Thermo Scientific) and EasySep monocyte purification kit (Stem Cell Technologies), respectively. Monocyte-derived myeloid dendritic cells (DCs)[22] were co-incubated at 2:1 ratio (T cell:monocyte) with 10 pmol/L antibodies for 5 days (Figure 1a). $CD14^+$ monocytes isolated from stimulator PBMCs were mixed with total $CD3^+$ T cells from PBMCs of HLA mismatched responders (1:3) (Figure 2d). IFN-γ was assessed in triplicates by MSD. For cytotoxicity, CMV-specific $CD8^+$T cells from CMV and HLA-A2 positive donors were isolated using pp65-loaded HLA-A2 tetramers and expanded *in vitro* using autologous DCs for 14 days.[22] K562 cells, transduced with an HLA-A2-coding lentivirus and sorted based on HLA-A2 expression, were further transduced with a lentiviral construct expressing PD-L1 (bystanders). The CMV pp65 protein and an IRES-GFP cassette under the EF1a promoter were introduced by lentiviral transduction to generate the K562-A2-CMV-PD-L1-pp65 targets. CMV+T cells were labeled with Cell Trace violet and were plated (2.5×10^4 cells/well) with tumor targets, bystanders (0.5:1:1), and antibodies for 2 days. GFP^+targets and GFP^-bystander cells were

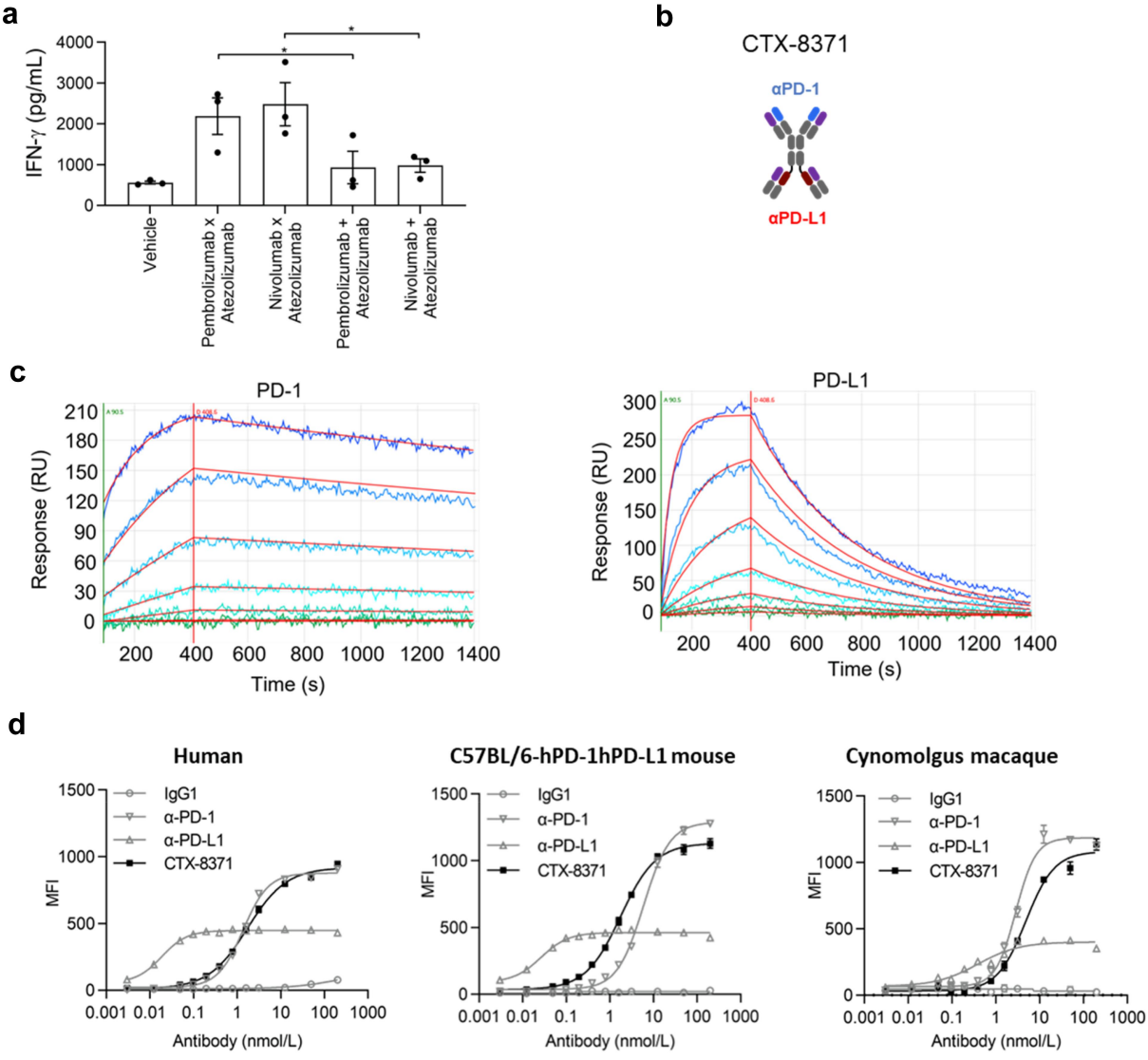

Figure 1. Discovery and binding profile of CTX-8371. (a) One-way MLR assay where monocyte derived DCs were used as stimulators and donor mismatched $CD4^+$T cells as responders. The activity of StitchMab™ bispecifics was compared to that of their unstitched combinations. IFN-γ was determined by MSD (mean ± SEM, $n = 3$) *, $p < 0.05$, one-way ANOVA. (b) CTX-8371 domain organization. (c) Sensorgrams of CTX-8371 binding to recombinant human PD-1 (left) and PD-L1 (right). The different curves correspond to determinations obtained with increasing concentrations of analyte (PD-1 or PD-L1, light to darker shades of blue). Red profiles represent the mathematical interpolation of the experimental data which was used to derive the kinetic parameters. (d) Binding of CTX-8371 to primary activated $CD3^+$ T cells from each species by FACS (mean ± SEM, $n = 3$).

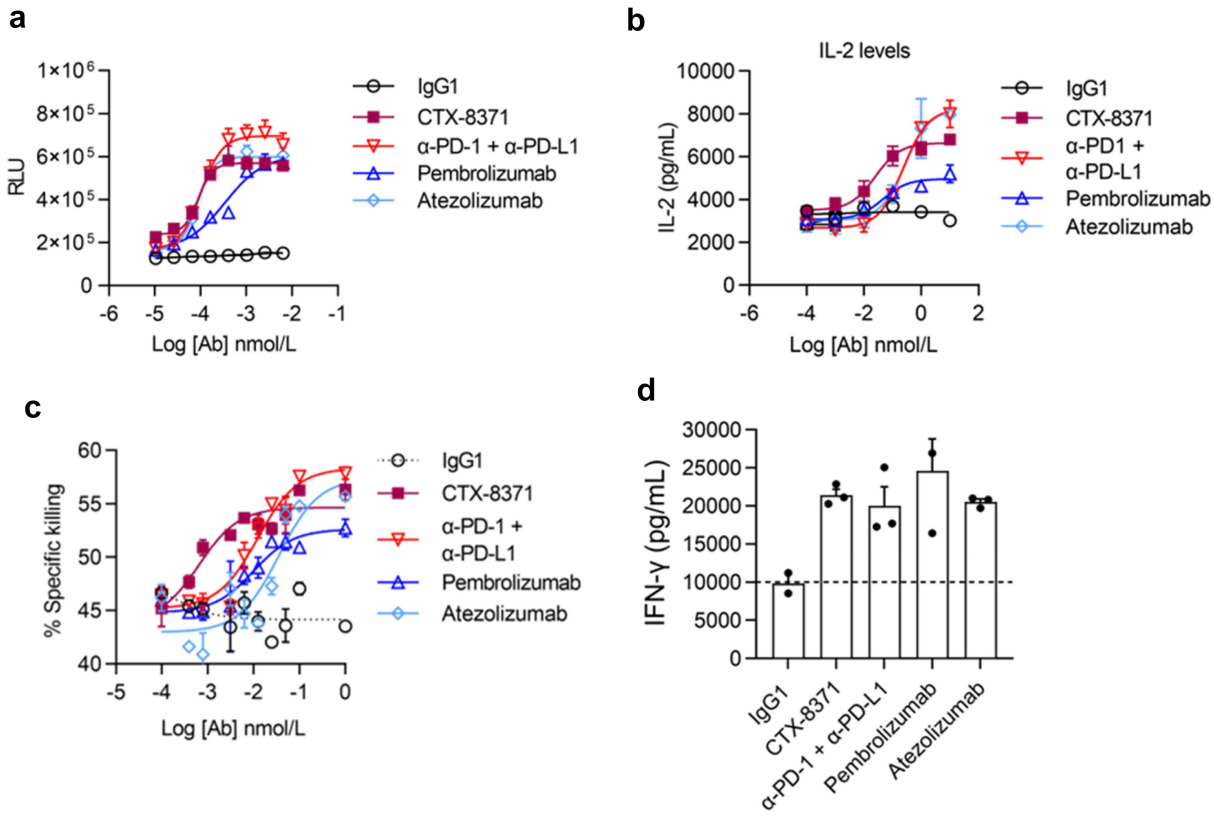

Figure 2. CTX-8371 enhances T cell function in primary human cells. (a) Jurkat-PD-1/NFAT-Luciferase reporter assay (mean ± SD; $n = 3$); (b) SEA polyclonal PBMC activation; (c) Antigen specific killing of tumor targets; (d) IFN-γ levels in the MLR (mean± SEM, $n = 3$). In this experiment, $CD14^+$ monocytes were used as stimulators and mismatched $CD3^+$ cells as responders.

enumerated after gating out the T cells, and specific killing was calculated as follows:

$$\%\ Specific\ killing = 100 * \left\{ 1 - \frac{\left[\frac{\%\ Targets+Tcells}{\%\ Bystanders+Tcells}\right]}{\left[\%\ \frac{Targets}{\%\ Bystanders}\right]} \right\}$$

Jurkat T cell reporter assay

TCR activation following receptor-ligand blockade was evaluated using the PD-1/PD-L1 Blockade Bioassay kit per manufacturer's recommended protocol (Promega). In this assay, antibodies inhibition of the PD-1/PD-L1 axis results in the increase of a luminescent reporter.

Jurkat cells experiments

Jurkat-PD-1 and Jurkat-PD-L1 (1:1) or Jurkat and Jurkat-PD-1/PD-L1 (1:1) were cocultured (1×10^6 cells/well) overnight in the presence of test antibodies. Half of the cells were processed for FACS using a CTX-8371 noncompetitive fluorescently labeled anti-PD-1 mAb, and half were processed for WB. PD-1 ECD levels were determined in supernatants collected at 0, 2, 4, 6, and 16 h. In some experiments, batimastat or MG132 (Sigma) were added 30 min in advance. Jurkat cells expressing either PD-1 or PD-L1 were labeled with 1 mmol/L CellTracker Green and CellTracker Red, respectively mixed (1:1, 1×10^6 cells/well), and cocultured in the presence of 1 nmol/L antibodies. Images were acquired at 0, 4 and 14 h with the IncuCyte® instrument (Sartorius).

In vivo studies

C57BL/6-*Pdcd1*$^{tm1(hPDCD1)}$ *Cd274*$^{tm1(hCD274)}$/Bcgen (C57BL/6-hPD-1hPD-L1) mice, harboring human/mouse chimeric PD-1 and PD-L1 were from Biocytogen. Experiments were conducted with 6–10-week-old female mice. For the tumor isograft studies, mice were inoculated with 1×10^6 tumor cells s.c. in the flank. Tumor volume (mm^3) was calculated as (Lx2W)/2, where L and W are the respective length and width measurements (mm). Tumor-bearing mice were randomized in groups and administered mAbs treatment i.p., in sterile PBS at 10 mg/Kg or CTX-8371 at the molar equivalent, 16 mg/Kg. Percent tumor growth inhibition (%TGI) was calculated on day 27 when the first 100% TGI (tumor-free mouse) occurred, using the following formula:

$$\%\ TGI = \frac{Largest\ TVol\ before\ Day\ 27 - TVol\ Day\ 27}{Largest\ TVol\ before\ Day\ 27} * 100$$

For CTX-8371/anti-CD137 combination, the mouse cross-reactive anti-CD137 antibody[23] was administered Q7Dx2 at 1.25 mg/kg. For the MC38-hPD-L1 re-challenge, tumor-free mice were paired with age-matched naïve controls and injected with 1×10^6 tumor cells, on the opposite flank. Mice in the B16F10-hPD-L1 melanoma metastases model in Figure 3e

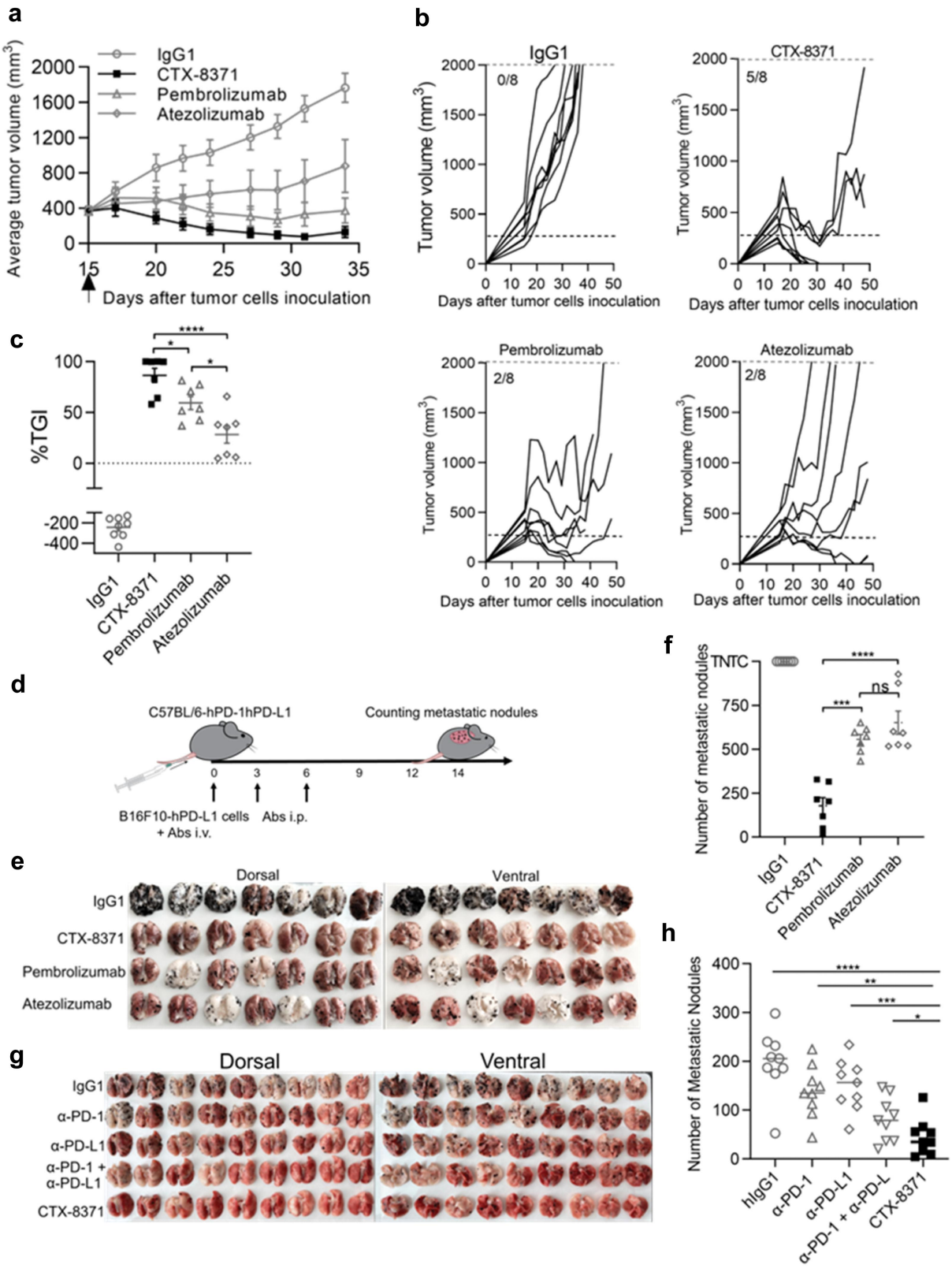

Figure 3. CTX-8371 anti-tumor activity *in vivo*. (a) Average tumor volume over time (mean ± SEM, $n = 8$). (b) Individual tumor growth curves. (c) %TGI on Day 27 (mean ± SEM, $n = 7$). ****, $p < 0.0001$, *, $p < 0.05$, one-way ANOVA, Tukey's multiple comparisons test. (d) Experimental design for lung metastasis prevention study. (e, g) Lungs, 15 (e) or 14 (g) Days after tumor cell injection and treatment. (f) Number of metastatic nodules in individual lungs (mean ± SEM, $n = 7$), ***, $p = 0.001$, one-way ANOVA and Tukey's multiple comparisons test. The lung nodules in control mice were too numerous to count (TNTC) and were excluded from the statistical analysis. (h) Number of lung metastatic nodules in individual mice (mean ± SEM, $n = 9$). **, $p < 0.01$, one-way ANOVA.

received 3×10^5 cells, whereas mice in Figure 3g received 1×10^5 cells i.v. together with the first dose of antibody. Next two doses were administered 3 days apart. On day 15 (Figure 3e) or 14 (Figure 3g), mice were euthanized, lungs were perfused with PBS, collected, and lung metastases counted by two independent operators. The lung nodules were distributed in three categories according to their size with a corresponding score of 1, 3 or 5, and counted. For immunophenotyping, groups of 4 mice bearing MC38-hPD-L1 tumors were injected i.v. with CTX-8371 at 0.1, 1, or 10 mg/kg, or vehicle. Single cell suspensions were prepared from tumors on days 1, 3, and 7, processed and analyzed by FACS. For PD-1 surface expression, groups of 6 mice bearing MC38-hPD-L1 tumors were injected i.v. with 10 mg/kg of CTX-8371 or IgG1. PBMCs and single cell suspensions prepared from tumors, tumor-draining lymph nodes, and spleen on days 3 and 6 were processed and analyzed by FACS.

Statistical analysis

GraphPad Prism v9.2 was used for all statistical analyses. $p < 0.05$ was considered significant.

Results

Discovery and binding profile of the anti-PD-1/PD-L1 bispecific antibody CTX-8371

Bispecific constructs of FDA approved antibodies in the StitchMab^{TM} format were tested in MLR. Pembrolizumab x atezolizumab and nivolumab x atezolizumab Stitchmabs emerged as the strongest IFN-γ inducers and were more potent than the combination of their parental antibodies (Figure 1a). This result prompted the generation of CTX-8371, a bispecific, tetravalent antibody composed of an anti-PD-1 aglyco-IgG1 with the Fab of anti-PD-L1 (heavy + light chain) fused at the C-terminus of each of its heavy chains through a glycine-serine $(G4S)_4$ linker (Figure 1b). The anti-PD-1 IgG1 and anti-PD-L1 Fab share a common light chain, which greatly simplifies its manufacturability. The IgG1 Fc of CTX-8371 is aglycosylated to abrogate effector functions. Single-step protein A purification yielded highly homogeneous material (>98% monomer by HPLC-SEC) and the final producing cell line exceeded industry standards. The affinity of CTX-8371 to recombinant human PD-1 and PD-L1 was determined as 3.8 nmol/L and 17.3 nmol/L respectively (Figure 1c). CTX-8371 affinity for recombinant murine PD-1 and PD-L1 proteins was 179-fold and 7.7-fold lower than human targets, therefore the molecule was deemed not suitable for testing in mice (Table S1). CTX-8371 bound with similar, low nanomolar affinity, to both human and cynomolgus monkey PD-1 and PD-L1 orthologs (Table S1). Binding to cell surface PD-1 and PD-L1 was evaluated on activated primary human or cynomolgus monkey PBMCs, murine C57BL/6-hPD-1hPD-L1 transgenic T cells, or CHO cells expressing ectopic human PD-1 or PD-L1. CTX-8371 bound to primary cells of human, mouse, and monkey origin, with comparable EC50 values (Figure 1d, table S2). Binding data using CHO cells overexpressing human PD-1 or PD-L1 showed CTX-8371 binding to the targets with similar avidity as the monoclonal anti-PD-1 or anti-PD-L1 parental antibodies, with EC50 values in the nanomolar range (Figure S1, table S2).

In vitro functional characterization of CTX-8371

To assess PD-1 blocking activity, we used an NFAT-Luciferase reporter assay in which disruption of the PD-1:PD-L1 interaction was followed by an increase in the activity of the reporter. In this setting, sub-nanomolar concentrations of CTX-8371 had similar potency as combination of parental anti-PD-1 and anti-PD-L1 mAbs. CTX-8371 blocking activity was comparable to an in-house generated atezolizumab-similar antibody (referred to as atezolizumab), but superior to pembrolizumab (Figure 2a). We next tested the effect of CTX-8371 inhibition in SEA-activated PBMCs. CTX-8371 induced a dose-dependent IL-2 increase 1.8-fold more potent than pembrolizumab, and 9-fold more potent than atezolizumab or the combination of CTX-8371's parental anti-PD-1 and PD-L1 antibodies (Figure 2b). Moreover, CTX-8371 more potently killed tumor cells expressing the CMV peptide compared to either the combined CTX-8371 parental mAbs or pembrolizumab (Figure 2c). In standard MLRs, CTX-8371 inhibitory activity was comparable to the activity of pembrolizumab and atezolizumab and their combination (Figure 2d).

CTX-8371 provides enhanced *in vivo* anti-tumor activity

Anti-tumor efficacy of CTX-8371 was investigated against solid tumors grown in transgenic C57BL/6-hPD-1hPD-L1 mice in which the inhibitory PD-1/PD-L1 signaling axis is functional, and PD-1 or PD-L1 blockade leads to regression of MC38-hPD-L1 colon tumors.[24] C57BL/6-hPD-1hPD-L1 mice bearing approximately 400 mm^3 MC38-hPD-L1 s.c. isografts received three doses of antibodies on days 15, 18, and 21 post tumor cell inoculation. CTX-8371 was highly effective and superior to both pembrolizumab and atezolizumab in controlling tumor growth (Figure 3a,b). The individual tumor growth Inhibition on day 27%TGI) was significantly higher (Figure 3c). In this model, pembrolizumab yielded two complete responses (25%) as did atezolizumab, albeit only transiently. CTX-8371 treatment led to durable tumor regression in 5 out of 8 mice (62.5%) (Figure 3b). Next, we tested whether the *in vivo* advantage of CTX-8371 was maintained in the more aggressive model of melanoma lung metastases B16F10-hPD-L1, where both tumor cells and antibodies were administered intravenously (Figure 3d). In this setting, CTX-8371 demonstrated significantly greater efficacy in preventing lung metastases than both pembrolizumab and atezolizumab monotherapies (3.11- and 3.64-fold less metastatic lung lesions) (Figure 3e,f). Since CTX-8371 was superior to the combination of the parental mAbs *in vitro* (Figures 2b,c), we assessed how this translated *in vivo*. Compared to isotype control (IC), each of the mAbs alone provided modest protection against B16F10-hPD-L1 metastases (1.46- and 1.32-fold fewer metastases respectively for anti-PD-1 and anti-PD-L1 mAbs), while their combination resulted in a significant 2.56-

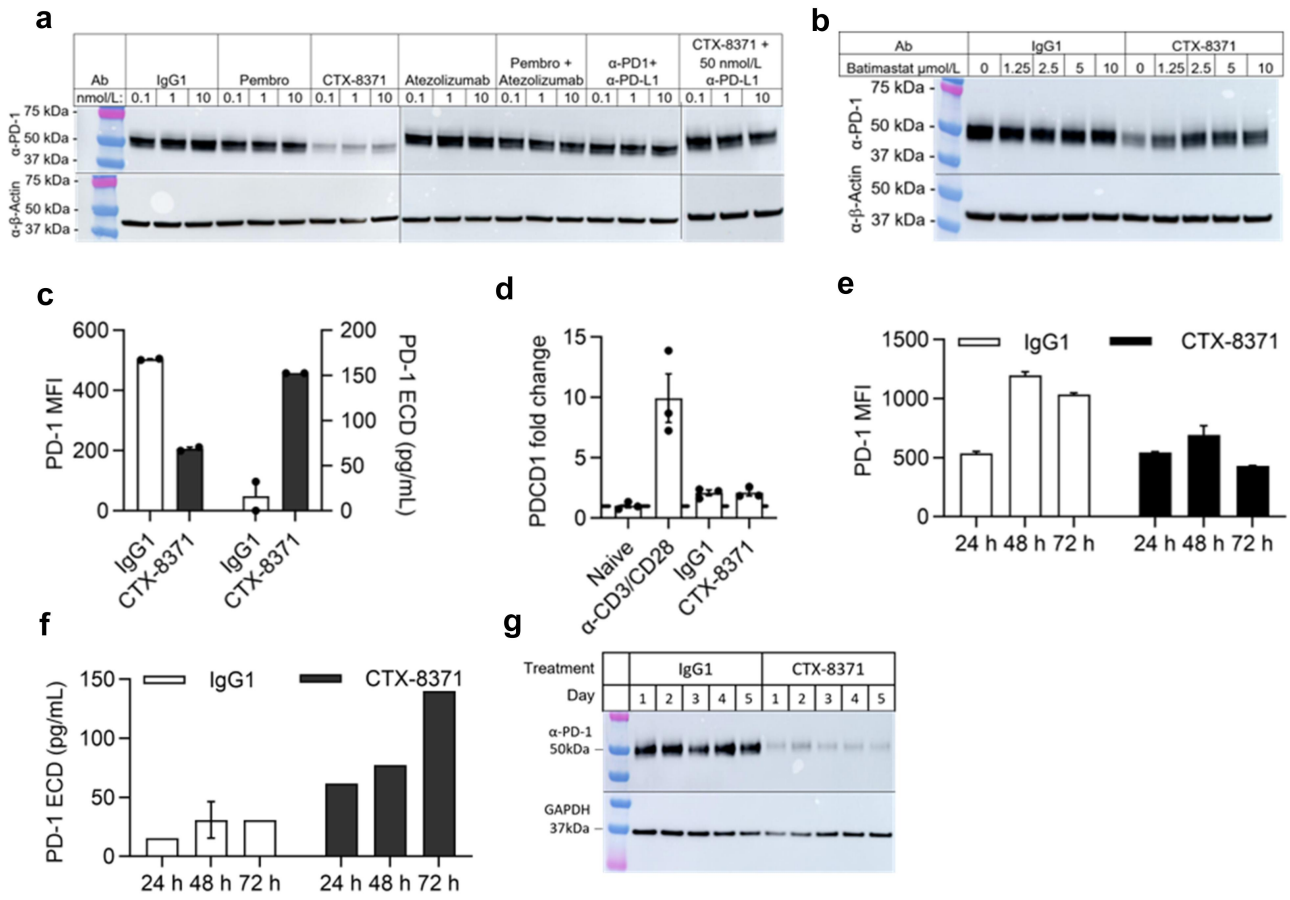

Figure 4. CTX-8371 promotes the loss of PD-1 in T cells. (a) PBMCs were stimulated with anti-CD3/CD28 for 72 h and treated overnight with antibodies. Endogenous levels of total PD-1 protein were detected by WB using a commercial rabbit monoclonal antibody directed against the intracellular domain of PD-1. (b) WB of PBMCs from (a), treated with antibodies overnight ± increasing concentrations of batimastat. (c) PD-1 surface expression and levels of PD-1 ECD in the supernatant of PBMCs stimulated as in (a) and treated overnight with antibodies (mean ± SEM, $n = 2$). *, $p < 0.05$, ***, $p < 0.005$, unpaired t test. (d) PDCD1 fold change compared to naive PBMCs of PBMCs activated with anti-CD3/CD28 for 72 h and activated PBMCs treated with antibodies overnight in the absence of anti-CD3/CD28. (e, f) PBMCs were stimulated for 72 h with anti-CD3/CD28 in the presence of IgG1 or CTX-8371. PD-1 surface expression (e) and PD-1 ECD (f) were determined every 24 h (mean ± SEM, $n = 2$). ****, $p < 0.0001$ for PD-1 MFI, ***, $p < 0.005$ for PD-1 ECD, two-way ANOVA. (g) 4 day-stimulated PBMCs were incubated overnight with antibodies, washed and restimulated with anti-CD3/anti-CD28 for 5 more days. The 5-day kinetics of PD-1 loss by WB after overnight exposure to CTX-8371. Pembro, pembrolizumab.

fold reduction in the number of metastatic nodules (Figure 3g, h). CTX-8371 was superior to all treatment groups showing a 5.37-fold reduction in metastatic nodules, with some animals presenting barely visible lesions. CTX-8371 treatment also resulted in 2.1-fold fewer nodules than the monoclonal antibody combination-treated mice (Figure 3g,h). The results suggest that additional mechanisms besides the blockade of PD-1: PD-L1 interaction might influence the activity of CTX-8371.

CTX-8371 drives sustained loss of surface PD-1 by proteolytic cleavage

One such mechanism might be PD-1 and/or PD-L1 down-regulation in response to CTX-8371 treatment. To test this, anti-CD3/anti-CD28-activated PBMCs were cultured with antibodies and PD-1 expression was determined by WB. PBMCs incubated with CTX-8371, but not IC or other antibodies targeting PD-1 or PD-L1, alone or in combination, demonstrated a substantial loss of PD-1 (Figure 4a). A bispecific bivalent anti-PD-1/anti-PD-L1 antibody (in which only one Fab' bound to each target) induced PD-1 loss, albeit less potently (Figure S2A). Pre-treatment with anti-PD-L1 prevented CTX-8371-induced PD-1 loss (Figure 4a), suggesting that both the *N*- and C-terminal ends of CTX-8371 must be engaged for PD-1 loss to occur. Notably, co-engagement of PD-1 and PD-L1 by CTX-8371 did not affect PD-L1 (Figure S2B). An approximately 15 kDa band, likely corresponding to the cleaved intracellular domain of PD-1, was consistently present in samples treated with CTX-8371 (Figures S2B-D, S3B). We tested whether ubiquitin/proteasomal or endosomal/lysosomal protein degradation pathways were involved in cleaving PD-1, by treating the stimulated cells with inhibitors of these pathways and examining whether they prevented the loss of PD-1. The proteasome inhibitor epoxomicin did not rescue the CTX-8371-mediated PD-1 loss (Figure S2C). We next tested whether the endo-lysosomal pathway was involved in the CTX-8371-mediated cleavage of PD-1. Treatment with chloroquine, which inhibits lysosomal proteases by preventing lysosomal acidification, did not rescue the PD-1 loss induced by CTX-8371 (Figure S2D). Chloroquine, however increased the intensity of the ~ 15kDa band, indicating that the intracellular PD-1 fragment might undergo lysosomal degradation. Since CTX-8371 did not induce PD-1 shedding via the intracellular or the

internalization routes, we hypothesized that PD-1 loss might be occurring extracellularly. Increasing concentrations of batimastat, a broad-spectrum protease inhibitor, were added to the IC or CTX-8371-treated samples. Batimastat rescued PD-1 loss in a dose-dependent manner indicating that an extracellular protease is involved (Figure 4b). PD-1 cleavage was confirmed by FACS (Figure 4c left, E) and using an ELISA method developed to specifically detect the N-terminal PD-1 fragment. The extracellular domain of PD-1 (referred to as PD-1 ECD) but not full-length PD-1 accumulated in the supernatant of CTX-8371-treated PBMC (Figure 4c right, 4F, S2E, and not shown). To test the possibility that CTX-8371 transcriptionally downregulates the expression of PDCD1 gene, mRNA levels of PD-1 were measured. It was found that PDCD1 mRNA levels were similar in activated human PBMCs treated with CTX-8371 or IC (Figure 4d). Finally, we asked whether PD-1 loss was transient or durable, by removing CTX-8371 after TCR stimulation while continuing the incubation with anti-CD3/anti-CD28 and sampling the cells for WB every day for 5 days. Overnight exposure to CTX-8371 but not IC resulted in a marked decrease in PD-1, which was not replenished for up to 5 days of additional stimulation (Figure 4g). These findings indicate that CTX-8371 promotes the shedding of the PD-1 protein expressed within days after TCR stimulation. Continuous cell stimulation after CTX-8371 removal neither resumed PD-1 expression nor increased it on the IC-exposed cells. Thus, exposure to CTX-8371 results in durable proteolytic cleavage of PD-1 from the cell surface and the release of PD-1 ECD.

PD-1 shedding occurs when CTX-8371 co-engages PD-1-expressing with PD-L1- expressing cells

Since co-engagement of PD-1 and PD-L1 produced a loss of PD-1 in a mixed population of cells, we asked whether PD-1 shedding occurs when CTX-8371 binds PD-1 and PD-L1 targets expressed by different cells (*trans*), or by the same cell (*cis*). CTX-8371 mediated the loss of PD-1 on Jurkat cells when the targets were in *trans* but not in *cis* configuration (Figure 5a). PD-1 loss was dose-dependently prevented by batimastat, demonstrating that proteolytic cleavage occurred in Jurkat cells (Figure 5a, left). WB of mixed Jurkat cell lysates confirmed that PD-1 loss occurred mainly *in trans* (Figure 5b). Batimastat prevented PD-1 cleavage in a dose-dependent manner (Figure 5b left) whereas proteasome inhibition did not rescue PD-1 loss from the cell surface (Figure S3). The rescue of PD-1 was also shown by the simultaneous disappearance of the 15 kDa band (Figure 5b, left). PD-1 ECD accumulation in the supernatant of *trans* configuration was dose dependent (Figure 5c, left) and there was no significant increase of PD-1 ECD in *cis* configuration (Figure 5c, right). We next visualized the interaction between Jurkat-PD-1 and Jurkat-PD-L1 cells in the presence of various antibodies by live imaging. Combination of the parental antibodies or pembrolizumab resulted in a minimal increase in the size of the cell clusters over time (Figure 5d). CTX-8371 led to the formation of large cell clusters, as early as 4 hours, and growing for up to 14 hours. These results suggest that CTX-8371 can bridge PD-1- with PD-L1-expressing cells, leading to a sustained loss of cell surface PD-1 and its accumulation in the supernatant.

CTX-8371-mediated efficacy is dose-dependent, relies on $CD8^+$ tumor-infiltrating lymphocytes (TILs) and correlates with PD-1 loss from TILs

We determined whether PD-1 loss occurred *in vivo* by analyzing the phenotype of MC38-hPD-L1 tumor infiltrating $CD8^+$ T cells. Compared to control, CTX-8371 enhanced the number of $CD45^+$ cells, including $CD8^+$ T cells which are the main effector cells in this model[25] (Figure 6a,b). CTX-8371 at 10 mg/kg enhanced the number of $CD45^+$ cells in a dose-dependent manner on day 7 after dosing when these cells also accumulated in higher numbers compared to days 1 and 3 (Figure 6b). Likewise, $CD8^+$ T cells infiltrated tumors in a dose-dependent manner on day 7 and in significantly higher numbers compared to both day 1 and 3. $CD8^+$ T cells already reached significant infiltrating numbers on day 3 after 10 mg/kg dosing. In addition, tumor-infiltrating $CD8^+$T cells on day 7 were significantly enriched by 1 mg/kg of CTX-8371 compared to day 1 (Figure 6b).

To study PD-1 expression *in vivo* we analyzed the phenotype of TILs on days 3 and 6 after 10 mg/kg single dose of CTX-8371. Percentages of PD-1^+ populations of $CD4^+$ and $CD8^+$ TILs, were significantly reduced on day 3 and remained reduced through day 6 (Figure 6c,d data not shown). Furthermore, the TILs infiltration and PD-1 loss correlated with the biological anti-tumor response. CTX-8371 treatment of MC38-hPD-L1 tumor-bearing mice resulted in a complete and durable anti-tumor response in 45% (4 of 9) of mice dosed with 10 mg/kg and 33% (3 of 9) of mice dosed with 1 mg/kg. No tumor regression was observed at 0.1 mg/kg (Figure S4A). Thus, 1 mg/kg was the lowest dose of CTX-8371 capable of inducing complete responses.

To examine the effect of CTX-8371 treatment on systemic levels of PD-1 protein, percentages of PD-1^+CD4^+ and PD-1^+CD8^+ T cells were assessed in mouse blood, tumor-draining lymph nodes, and spleen. Significant reductions in frequencies of these cells were detected on day 3 after treatment in the secondary lymphoid organs but not in circulation (Figure 4Sb). On day 6, the PD-1^+ T cell frequencies were reduced in lymph nodes, spleen, and in PBMCs (Figure 6e). Based on the kinetics of PD-1 shedding, CTX-8371 appeared to facilitate PD-1 loss more efficiently in organized lymphoid tissues than in circulation. Thus, CTX-8371 treatment resulted in a global reduction of PD-1 protein in tumor-bearing mice. Overall, the PD-1 loss appeared more durable in CD4 than CD8 T cells.

CTX-8371 drives PD-1 loss on cynomolgus macaques peripheral T lymphocytes

To assess whether the loss of cell surface PD-1 could be used as PD biomarker, we analyzed the surface levels of PD-1 on $CD4^+$ and $CD8^+$ T cells of cynomolgus macaques one day after CTX-8371 treatment. Almost complete CTX-8371-mediated loss in the frequency of PD-1^+ T cells and significantly lower expression of PD-1 was observed in peripheral blood compared to pre-treatment values in all treatment groups, while the total $CD4^+$ or $CD8^+$ T cell percentages did not change (Figure 7). Altogether, the data show that CTX-8371 treatment produces a long-lasting PD-1 loss in human T cells treated *in vitro*, in tumor-bearing mice, and peripheral blood T cells from treated non-human primates.

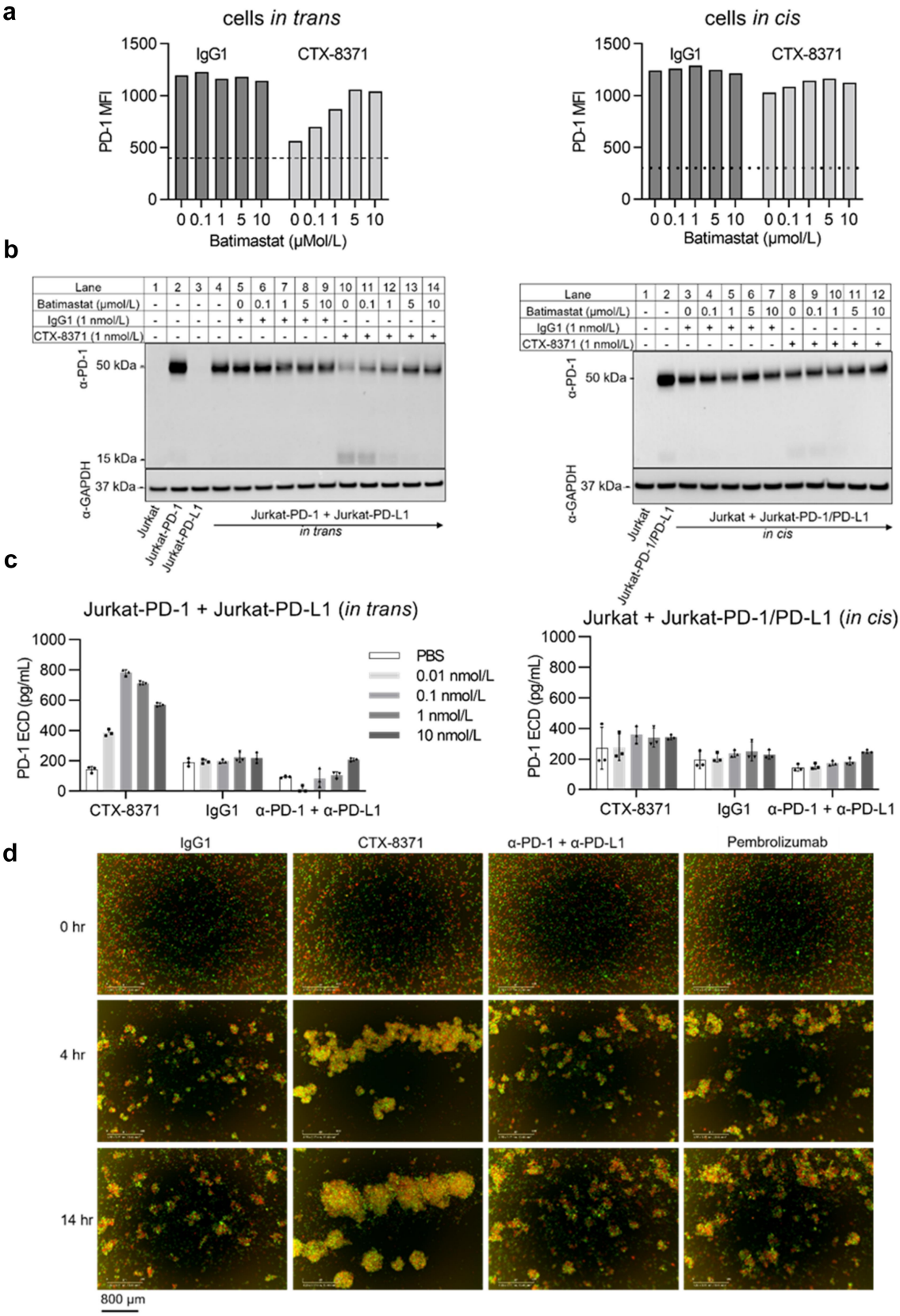

Figure 5. Loss of PD-1 by CTX-8371 occurs *in trans* and requires proteolytic activity. (a) *Trans* or *cis* Jurkat systems were treated with antibodies and increasing concentrations of batimastat. PD-1 expression by FACS is plotted as a function of batimastat concentration. Dotted lines represent the cut-off PD-1 expression on Jurkat-PD-L1 (left) or Jurkat parental cells (right). (b) WB of PD-1 expression in lysates of mixed Jurkat cells from (a). (c) PD-1 ECD levels in the mixed reactions (mean ± SD, $n = 3$). ****, $p < 0.0001$ between CTX-8371 and IgG1 or α-PD1+α-PD-L1 at all concentrations, one-way ANOVA and Tukey's multiple comparisons test. (d) Representative images of *trans* Jurkat cells by IncuCyte.

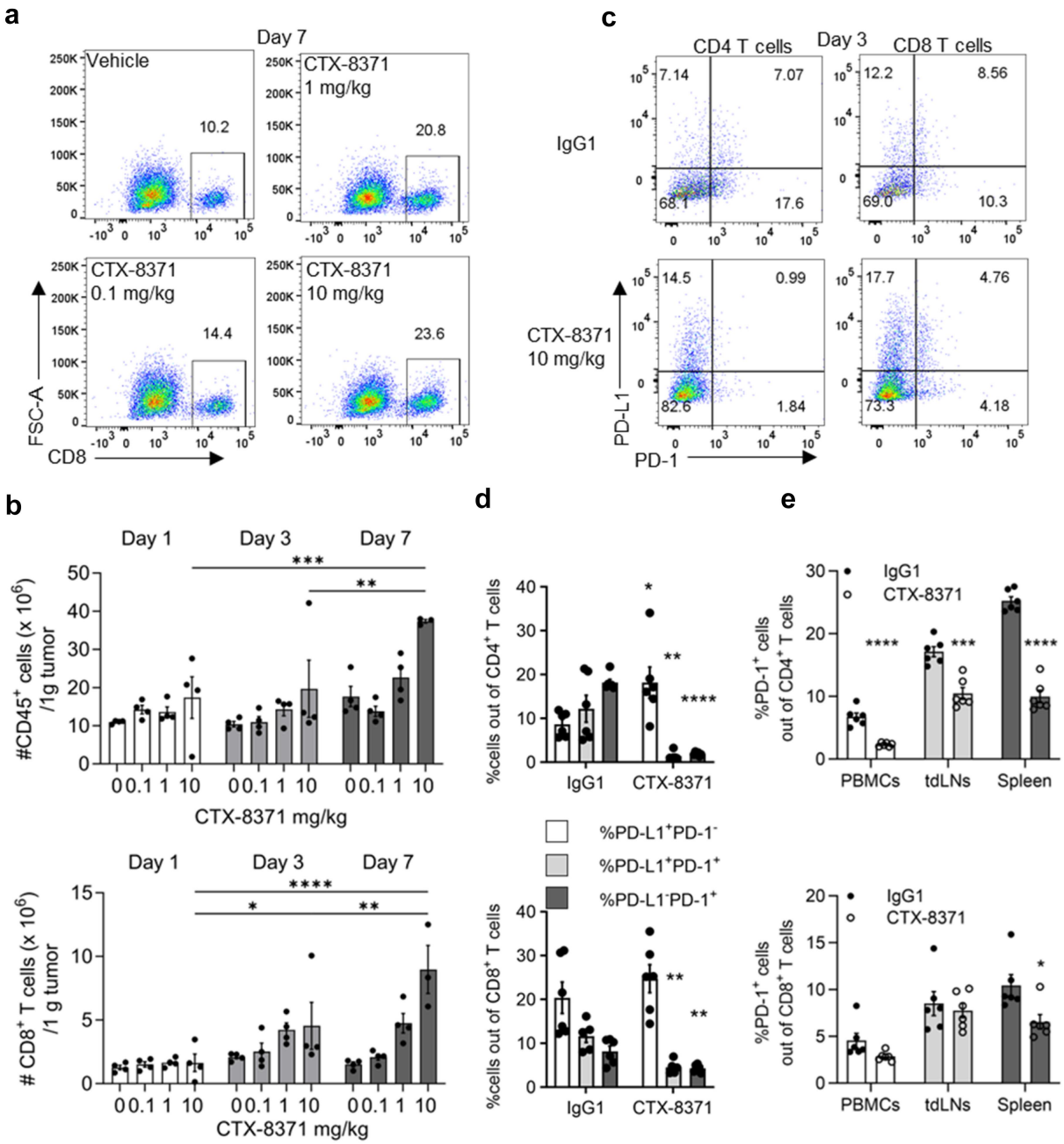

Figure 6. CTX-8371 causes CD8 T cell infiltration in tumors and global loss of PD-1 on T cells. mice received a single dose of CTX-8371. Spleen, tdLns, PBMCs, and tumor cell suspensions were analyzed by FACS. (A) $CD8^+$ T cells percentages out of $CD45^+$ immune cells on day 7. (B) Absolute numbers of $CD45^+$ (upper) and $CD8^+$T cells (lower) per gram of tumor tissue (mean ± SEM, $n = 4$), ****, $p < 0.0001$, ***, $p < 0.005$, **, $p < 0.001$, *, $p < 0.05$. Two-way ANOVA and Tukey's multiple comparisons test. (C) Representative dot plots of PD-1-expressing T cells on day 3 after dosing with CTX-8371 or IgG1. (D) $PD\text{-}1^+$ T cell frequencies in all tumors (mean ± SEM, $n = 6$). *, $p < 0.05$, **, $p < 0.001$, ***, $p < 0.005$, ****, $p < 0.0001$ unpaired t test. (E) CTX-8371 reduces PD-1 on $CD4^+$ and $CD8^+$ T lymphocytes in the periphery on day 6. (mean ± SEM, $n = 6$), ****, $p < 0.0001$, ***, $p < 0.005$, **, $p < 0.001$, *, $p < 0.05$ unpaired t test.

CTX-8371 curative anti-tumor efficacy in combination with anti-CD137 antibody

In addition to PD-1 loss, $CD8^+$ TILs in the MC38-hPD-L1 tumors treated with CTX-8371 markedly upregulated the expression of the costimulatory receptor CD137 and granzyme B, indicating activation (Figure 8a,b). This observation prompted the investigation of the efficacy of CTX-8371 in combination with an agonist anti-CD137 antibody. Mice bearing MC-38-hPD-L1 tumors were treated with CTX-8371 and a mouse cross-reactive variant of our clinical lead, CTX-471.[23] This treatment resulted in a dramatic enhancement of the anti-tumor effect, with tumor regressions occurring in all animals (Figure 8c,d). Tumor-free mice from the CTX-8371 and the combination groups were observed for 30 days without any relapse indicating that CTX-8371 alone or in combination led to durable tumor regression. Mice were subsequently re-challenged with MC38-hPD-L1 tumor cells. No tumor grew in any of the CTX-8371 and CTX-8371+ anti-CD-137 cured mice during a three-week observation phase, whereas tumors grew in all naïve control mice (Figure 8e). This indicated a strong protective immunological memory elicited by the first tumor challenge.

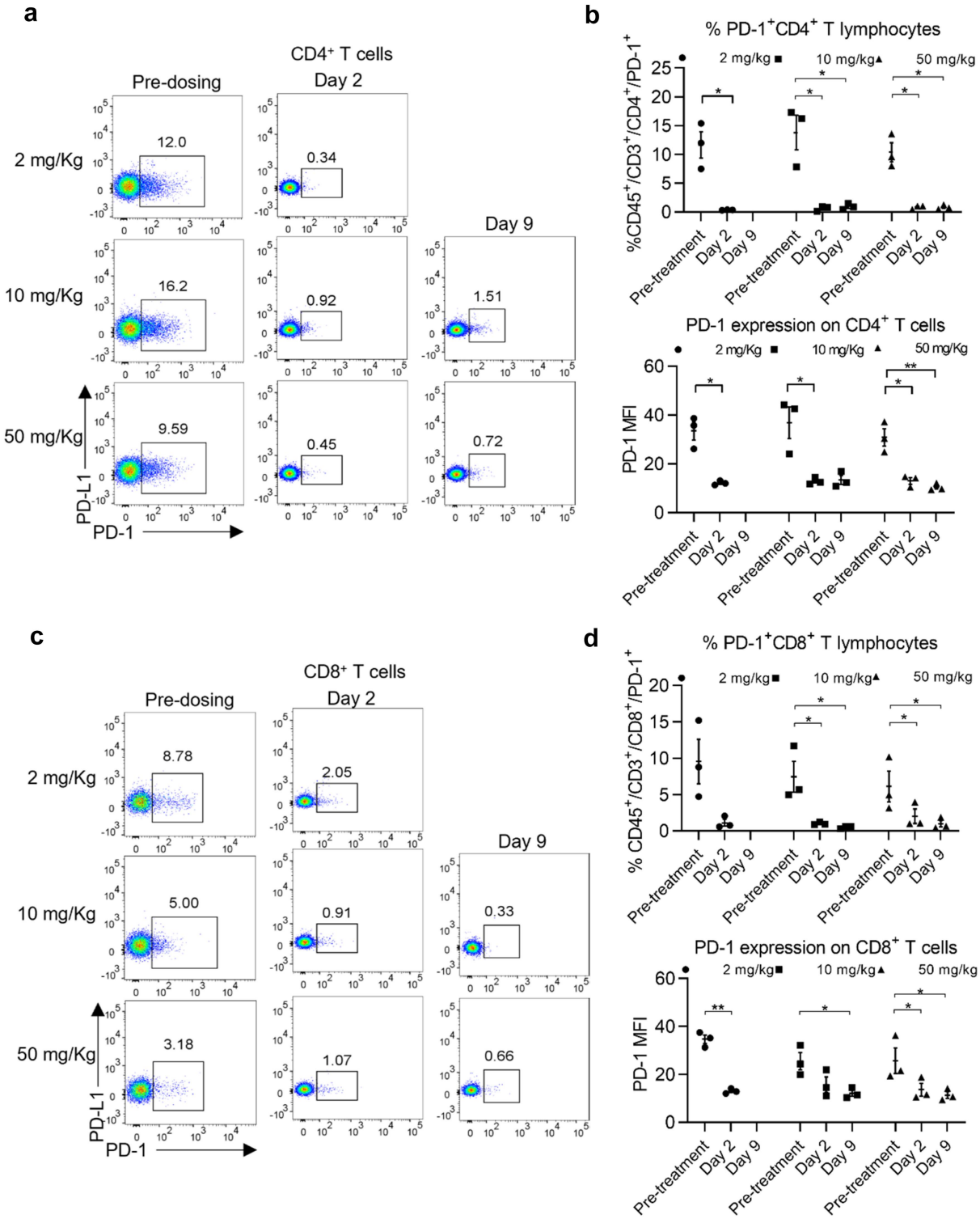

Figure 7. CTX-8371-mediated loss of PD-1 on peripheral T lymphocytes of cynomolgus monkeys. (a, c) Representative dot plots of monkey PD-1$^+$ CD4$^+$ and CD8$^+$ T cells at pre-treatment and on days 2 and 9 after CTX-8371 dosing. (b, d) peripheral blood PD-1$^+$ CD4$^+$ and CD8$^+$ T cell frequencies and PD-1 MFI in all monkeys (mean ± SEM, $n = 3$). **, $p < 0.001$, *, $p < 0.05$, one-way ANOVA and Dunnett's multiple comparisons test.

Discussion

We presented compelling evidence that co-targeting of PD1 and PD-L1 with a bispecific tetravalent Ab outperforms mAbs in a series of *in vitro* and *in vivo* experimental settings. These results were not anticipated since both arms of CTX-8371 inhibit the same receptor:ligand interaction, the PD-1:PD-L1 signaling axis. Slight advantages for CTX-8371 were predicted over mAbs, as blocking PD-1 can also affect the interaction of PD-1 with PD-L2 and blocking PD-L1 may have liberated CD80 costimulatory molecule.[26] Increased benefit of blocking the PD-1:PD-L1 receptor:ligand interaction using combinations of mAbs *in vivo* has been reported before[27,28] and, more recently, the activity of bivalent bispecific molecules co-

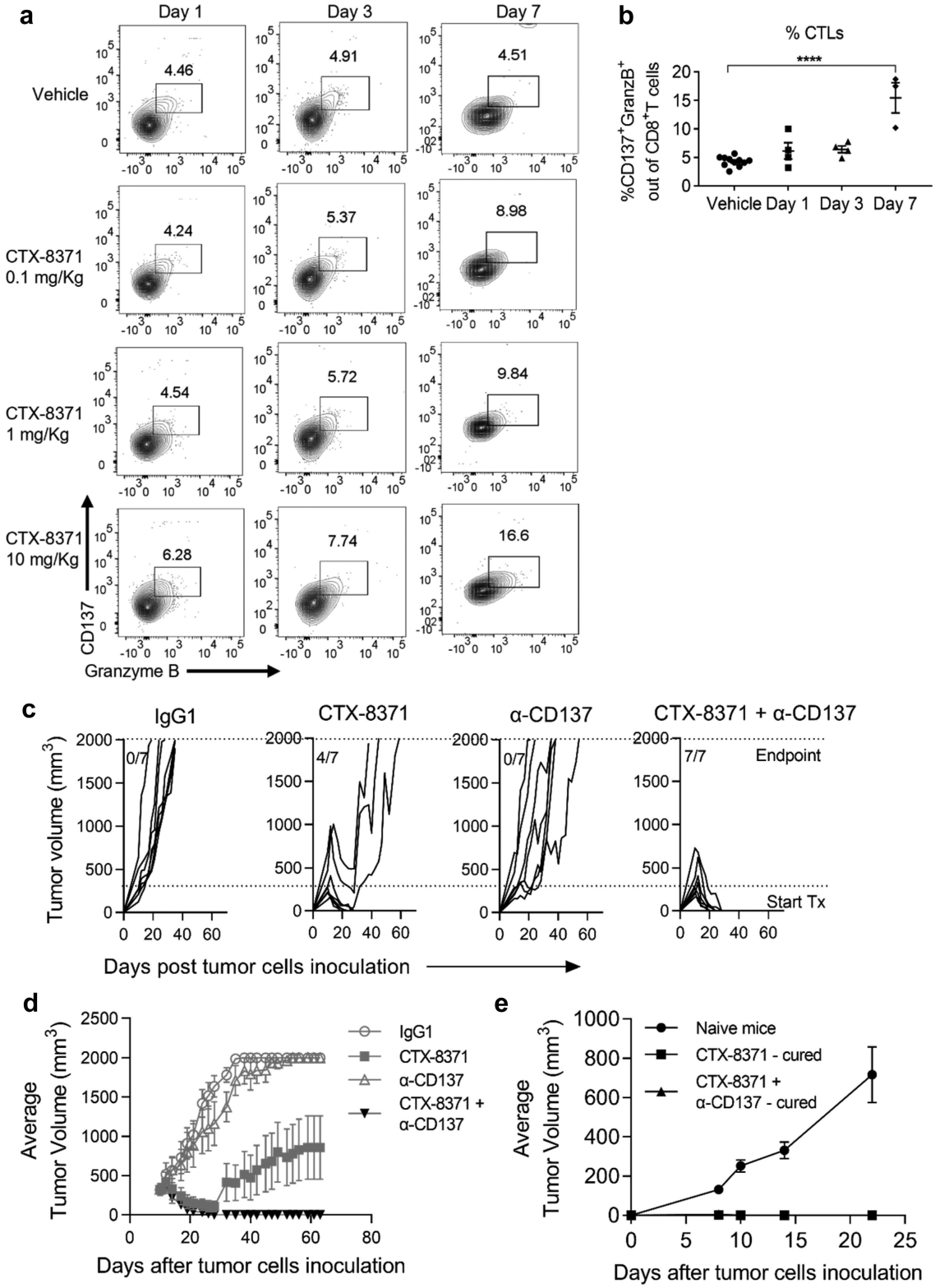

Figure 8. Anti-tumor efficacy of CTX-8371 in combination with anti-CD137 antibodies. (a) Representative contour plots for each dose and time point showing CTL frequencies, gated on $CD8^+$ T cells. (b) $CD137^+$Granzyme B^+CD8^+ T cell frequencies in the 10 mg/kg and control (mean ± SEM, $n = 4$). ****, $p < 0.0001$, **, $p < 0.001$, *, $p < 0.05$. One-way ANOVA and Dunnett's multiple comparisons test. (c) Individual tumor growth curves ($n = 7$) (d) Average tumor volume (mm^3) for each treatment group. (e) MC38-hPD-L1 tumor growth plot of re-challenged tumor-free and naïve control mice (mean ± SEM, $n = 4$–10).

targeting PD-1 and PD-L1 has also been disclosed.[29] Given the enhanced activity of the bispecific constructs, we asked whether additional mechanisms could have conferred the functional advantage. We discovered that CTX-8371 induced proteolytic stripping of the extracellular domain of PD-1 in polyclonally stimulated T cells. This occurred only when CTX-8371 co-engaged PD-1 and PD-L1 expressed on different cells. Our studies suggest a model in which CTX-8371 binding to

PD-L1 may facilitate the reorientation of PD-1 ECD resulting in the exposure of a protease recognition site in the PD-1 stalk region, which would trigger the shedding of PD-1 from the cell surface. In support of this, a bispecific version of CTX-8371 in which only one Fab' bound to each target, induced shedding less potently. Whereas PD-L1 cleavage has been documented as a resistance mechanism,[30] CTX-8371 appears to uniquely facilitate cleavage of PD-1, which to the best of our knowledge is not known to be physiologically subjected to shedding. While the precise events initiated by CTX-8371 targets engagement have yet to be elucidated, the putative protease likely is T-cell derived since we observed cleavage in Jurkat cells. Potential candidates and known targets for batimastat are sheddases like MMPs or ADAMs. These enzymes have been involved in ectodomain shedding of numerous surface immunomodulators and other proteins.[31] Likely, the efficacy of CTX-8371 might be further enhanced *in vivo* by virtue of other proteases present in the tumor microenvironment (TME). These could amplify PD-1 loss if their specificity for PD-1 overlaps with that of the putative sheddase. The ability of CTX-8371 to bridge cells expressing PD-1 with cells expressing PD-L1 appears to be essential for exposing the proteolytic cleavage site. The kinetics of PD-1 loss, both in activated primary cells and in Jurkat cell *trans* system, indicates that the cleavage occurs within the time frame of cellular aggregation. It is tempting to speculate that the CTX-8371 might promote loss of PD-1 primarily where APCs and T cells interact (e.g. lymph nodes, spleens, tumors). This would be followed by the accumulation of PD-1 ECD,[32,33] which could act as a decoy soluble receptor for PD-L1, further amplifying its blockade of the PD-1/PD-L1 signaling axis.[33] Since PD-1 loss correlated with robust anti-tumor response, monitoring PD-1 ECD levels before and after treatment has the potential to serve as a pharmacodynamic biomarker for patients treated with CTX-8371. With the current tools, we were not able to reliably quantify PD-1 ECD in the serum of treated mice and monkeys. We are now developing better methods to test this hypothesis directly in the clinic.

Analysis of the PD-1 loss in the peripheral T cells of tumor-bearing mice and of treated healthy monkeys, suggests that shedding of PD-1 can occur in blood. It is conceivable that i.v. injected CTX-8371 may engage melanoma cells and circulating PD-1-expressing effector cells in the B16F10-hPD-L1 metastases model, explaining the superior efficacy of CTX-8371 over the standard blocking antibodies, and even their combination.

CTX-8371 outperformed FDA-approved antibodies in both the immunologically responsive MC38 colon carcinoma, and a classic model of "cold" TME, the B16F10 melanoma metastasis model and combination of CTX-8371 with anti-CD137 antibody resulted in long-lasting, complete anti-tumor responses. These findings offered a strong scientific rationale to pursue a therapeutic approach where PD-1 or PD-L1 targeting agents are combined with a CD137 agonist. We initiated the clinical evaluation of Keytruda® plus CTX-471, our anti-CD137 agonistic antibody[23] (NCT03881488). Combinations of CPIs have already shown enhanced therapeutic effect in melanoma and other malignancies[34–36] and the demand for novel immunomodulatory drugs continues to remain high. CTX-8371 may offer superior clinical benefit over single agents targeting the PD-1/PD-L1 pathway due to its novel differentiated and non-redundant mechanism of action. This potential could be further harnessed in combinatorial approaches with agents that target additional immunomodulatory receptors, such as CD137, or other orthogonal anti-cancer agents.

Acknowledgments

The authors wish to thank William "Beau" Carson and Kris Sachsenmeier for scientific discussions, Autumn Ruiz and Walter Rodriguez for vivarium & IACUC management and animal care respectively, Rachael Duffy for technical assistance, Jonathan Anderman, and Neil Schilling for critical review of the manuscript.

Disclosure statement

All the authors are current or former Compass Therapeutics Inc. employees and either owned or own equity in the company.

Funding

The author(s) reported there is no funding associated with the work featured in this article.

Author contributions

BW, YQ, XW, ADU, MS, ED, VL, JG, BG, DIA, and AV designed, conducted experiments, and analyzed data. XW, RJ, JK, and BG designed, produced, and characterized the antibodies, NK and TJS provided leadership, critically reviewed the manuscript, AV substantially revised the manuscript and DIA wrote the manuscript.

Data availability statement

The authors confirm that the data supporting the findings of this study are available within the article and its supplementary materials.

References

1. Agata Y, Kawasaki A, Nishimura H, Ishida Y, Tsubat T, Yagita H, Honjo T. Expression of the PD-1 antigen on the surface of stimulated mouse T and B lymphocytes. Int Immunol. 1996;8(5):765–772. doi:10.1093/intimm/8.5.765.
2. Hui E, Cheung J, Zhu J, Su X, Taylor MJ, Wallweber HA, Sasmal DK, Huang J, Kim JM, Mellman I. et al. T cell costimulatory receptor CD28 is a primary target for PD-1–mediated inhibition. Science. 2017;355(6332):1428–1433. doi:10.1126/science.aaf1292.
3. Nishimura H, Okazaki T, Tanaka Y, Nakatani K, Hara M, Matsumori A, Sasayama S, Mizoguchi A, Hiai H, Minato N. et al. Autoimmune dilated cardiomyopathy in PD-1 receptor-deficient mice. Science. 2001;291(5502):319–322. doi:10.1126/science.291.5502.319.
4. Freeman GJ, Long AJ, Iwai Y, Bourque K, Chernova T, Nishimura H, Fitz LJ, Malenkovich N, Okazaki T, Byrne MC. et al. Engagement of the PD-1 immunoinhibitory receptor by a novel B7 family member leads to negative regulation of lymphocyte activation. J Exp Med. 2000;192(7):1027–1034. doi:10.1084/jem.192.7.1027.
5. Dong H, Strome SE, Salomao DR, Tamura H, Hirano F, Flies DB, Roche PC, Lu J, Zhu G, Tamada K. et al. Tumor-associated B7-H1 promotes T-cell apoptosis: a potential mechanism of immune evasion. Nat Med. 2002;8(8):793–800. doi:10.1038/nm730.

6. Li K, Yuan Z, Lyu J, Ahn E, Davis SJ, Ahmed R, Zhu C. PD-1 suppresses TCR-CD8 cooperativity during T-cell antigen recognition. Nat Commun. 2021;12(1):2746. doi:10.1038/s41467-021-22965-9.
7. Yokosuka T, Takamatsu M, Kobayashi-Imanishi W, Hashimoto-Tane A, Azuma M, Saito T. Programmed cell death 1 forms negative costimulatory microclusters that directly inhibit T cell receptor signaling by recruiting phosphatase SHP2. J Exp Med. 2012;209(6):1201–1217. doi:10.1084/jem.20112741.
8. Ostrand-Rosenberg S, Horn LA, Haile ST. The programmed death-1 immune-suppressive pathway: barrier to antitumor immunity. J Immunol. 2014;193(8):3835–3841. doi:10.4049/jimmunol.1401572.
9. Kuchroo JR, Hafler DA, Sharpe AH, Lucca LE. The double-edged sword: harnessing PD-1 blockade in tumor and autoimmunity. *Sci Immunol*. 2021;6(65):eabf4034. doi:10.1126/sciimmunol.abf4034.
10. Wei SC, Duffy CR, Allison JP. Fundamental Mechanisms of Immune Checkpoint Blockade Therapy. Cancer Discov. 2018;8(9):1069–1086. doi:10.1158/2159-8290.CD-18-0367.
11. Brahmer JR, Tykodi SS, Chow LQM, Hwu W-J, Topalian SL, Hwu P, Drake CG, Camacho LH, Kauh J, Odunsi K. et al. Safety and activity of anti–PD-L1 antibody in patients with advanced cancer. N Engl J Med. 2012;366(26):2455–2465. doi:10.1056/NEJMoa1200694.
12. Topalian SL, Hodi FS, Brahmer JR, Gettinger SN, Smith DC, McDermott DF, Powderly JD, Carvajal RD, Sosman JA, Atkins MB. et al. Safety, activity, and immune correlates of anti–PD-1 antibody in cancer. N Engl J Med. 2012;366(26):2443–2454. doi:10.1056/NEJMoa1200690.
13. Yap TA, Parkes EE, Peng W, Moyers JT, Curran MA, Tawbi HA. Development of immunotherapy combination strategies in cancer. Cancer Discov. 2021;11(6):1368–1397. doi:10.1158/2159-8290.CD-20-1209.
14. Chae YK, Arya A, Iams W, Cruz MR, Chandra S, Choi J, Giles F. Current landscape and future of dual anti-CTLA4 and PD-1/PD-L1 blockade immunotherapy in cancer; lessons learned from clinical trials with melanoma and non-small cell lung cancer (NSCLC). J Immunother Cancer. 2018;6(1):39. doi:10.1186/s40425-018-0349-3.
15. Jerby-Arnon L, Shah P, Cuoco MS, Rodman C, Su M-J, Melms JC, Leeson R, Kanodia A, Mei S, Lin J-R. et al. A cancer cell program promotes T cell exclusion and resistance to checkpoint blockade. Cell. 2018;175(4):984–997 e924. doi:10.1016/j.cell.2018.09.006.
16. Weiss SA, Sznol M. Resistance mechanisms to checkpoint inhibitors. Curr Opin Immunol. 2021;69:47–55. doi:10.1016/j.coi.2021.02.001.
17. Nie S, Wang Z, Moscoso-Castro M, D'Souza P, Lei C, Xu J, Gu J. Biology drives the discovery of bispecific antibodies as innovative therapeutics. Antib Ther. 2020;3(1):18–62. doi:10.1093/abt/tbaa003.
18. Syed YY. Amivantamab: first approval. Drugs. 2021;81(11):1349–1353. doi:10.1007/s40265-021-01561-7.
19. Kang C. Mosunetuzumab: first approval. Drugs. 2022;82(11):1229–1234. doi:10.1007/s40265-022-01749-5.
20. Keam SJ. Cadonilimab: first approval. Drugs. 2022;82(12):1333–1339. doi:10.1007/s40265-022-01761-9.
21. Zakeri B, Fierer JO, Celik E, Chittock EC, Schwarz-Linek U, Moy VT, Howarth M. Peptide tag forming a rapid covalent bond to a protein, through engineering a bacterial adhesin. Proc Natl Acad Sci USA. 2012;109(12):E690–697. doi:10.1073/pnas.1115485109.
22. Sallusto F, Lanzavecchia A. Efficient presentation of soluble antigen by cultured human dendritic cells is maintained by granulocyte/macrophage colony-stimulating factor plus interleukin 4 and downregulated by tumor necrosis factor alpha. J Exp Med. 1994;179(4):1109–1118. doi:10.1084/jem.179.4.1109.
23. Eskiocak U, Guzman W, Wolf B, Cummings C, Milling L, Wu H-J, Ophir M, Lambden C, Bakhru P, Gilmore DC. et al. Differentiated agonistic antibody targeting CD137 eradicates large tumors without hepatotoxicity. JCI Insight. 2020;5(5). doi:10.1172/jci.insight.133647.
24. Park JJ, Thi EP, Carpio VH, Bi Y, Cole AG, Dorsey BD, Fan K, Harasym T, Iott CL, Kadhim S. et al. Checkpoint inhibition through small molecule-induced internalization of programmed death-ligand 1. Nat Commun. 2021;12(1):1222. doi:10.1038/s41467-021-21410-1.
25. Jin Y, An X, Mao B, Sun R, Kumari R, Chen X, Shan Y, Zang M, Xu L, Muntel J. et al. Different syngeneic tumors show distinctive intrinsic tumor-immunity and mechanisms of actions (MOA) of anti-PD-1 treatment. Sci Rep. 2022;12(1):3278. doi:10.1038/s41598-022-07153-z.
26. Butte MJ, Keir ME, Phamduy TB, Sharpe AH, Freeman GJ. Programmed death-1 ligand 1 interacts specifically with the B7-1 costimulatory molecule to inhibit T cell responses. Immunity. 2007;27(1):111–122. doi:10.1016/j.immuni.2007.05.016.
27. Burrack AL, Spartz EJ, Raynor JF, Wang I, Olson M, Stromnes IM. Combination PD-1 and PD-L1 Blockade promotes durable neoantigen-specific T Cell-mediated immunity in pancreatic ductal adenocarcinoma. Cell Rep. 2019;28(8):2140–2155 e2146. doi:10.1016/j.celrep.2019.07.059.
28. Ngiow SF, Young A, Jacquelot N, Yamazaki T, Enot D, Zitvogel L, Smyth MJ. A threshold level of intratumor CD8+ T-cell PD1 expression dictates therapeutic response to anti-PD1. Cancer Res. 2015;75(18):3800–3811. doi:10.1158/0008-5472.CAN-15-1082.
29. Kotanides H, Li Y, Malabunga M, Carpenito C, Eastman SW, Shen Y, Wang G, Inigo I, Surguladze D, Pennello AL. et al. Bispecific targeting of PD-1 and PD-L1 enhances T-cell activation and antitumor immunity. Cancer Immunol Res. 2020;8(10):1300–1310. doi:10.1158/2326-6066.CIR-20-0304.
30. Orme JJ, Jazieh KA, Xie T, Harrington S, Liu X, Ball M, Madden B, Charlesworth MC, Azam TU, Lucien F. et al. ADAM10 and ADAM17 cleave PD-L1 to mediate PD-(L)1 inhibitor resistance. Oncoimmunology. 2020;9(1):1744980. doi:10.1080/2162402X.2020.1744980.
31. Hayashida K, Bartlett AH, Chen Y, Park PW. Molecular and cellular mechanisms of ectodomain shedding. Anat Rec (Hoboken). 2010;293(6):925–937. doi:10.1002/ar.20757.
32. Fransen MF, Schoonderwoerd M, Knopf P, Camps MGM, Hawinkels LJAC, Kneilling M, van Hall T, Ossendorp F. Tumor-draining lymph nodes are pivotal in PD-1/PD-L1 checkpoint therapy. JCI Insight. 2018;3(23). doi:10.1172/jci.insight.124507.
33. Khan M, Zhao Z, Arooj S, Fu Y, Liao G. Soluble PD-1: predictive, prognostic, and therapeutic value for cancer immunotherapy. Front Immunol. 2020;11:587460. doi:10.3389/fimmu.2020.587460 .
34. Tawbi HA, Schadendorf D, Lipson EJ, Ascierto PA, Matamala L, Castillo Gutiérrez E, Rutkowski P, Gogas HJ, Lao CD, De Menezes JJ. et al. Relatlimab and nivolumab versus nivolumab in untreated advanced melanoma. N Engl J Med. 2022;386(1):24–34. doi:10.1056/NEJMoa2109970.
35. Nakajima EC, Vellanki PJ, Larkins E, Chatterjee S, Mishra-Kalyani PS, Bi Y, Qosa H, Liu J, Zhao H, Biable M. et al. FDA approval summary: nivolumab in combination with ipilimumab for the treatment of unresectable malignant pleural mesothelioma. Clin Cancer Res. 2022;28(3):446–451. doi:10.1158/1078-0432.CCR-21-1466.
36. Postow MA, Chesney J, Pavlick AC, Robert C, Grossmann K, McDermott D, Linette GP, Meyer N, Giguere JK, Agarwala SS. et al. Nivolumab and ipilimumab versus ipilimumab in untreated melanoma. N Engl J Med. 2015;372(21):2006–2017. doi:10.1056/NEJMoa1414428.